

Predicting seasonal influenza transmission using Regression Models with Temporal Dependence

Manuel Oviedo de la Fuente^{1,2*}, Manuel Febrero-Bande¹,
María Pilar Muñoz³ and Ángela Domínguez^{4,5}

October 28, 2016

Abstract

In this manuscript, we use meteorological information in Galicia (Spain) to propose a novel approach to predict the incidence of influenza. Our approach extends the GLS methods in the multivariate framework to functional regression models with dependent errors. A simulation study shows that the GLS estimators render better estimations of the parameters associated with the regression model and obtain extremely good results from the predictive point of view. Thus they improve the classical linear approach. It proposes an iterative version of the GLS estimator (called iGLS) that can help to model complicated dependence structures, uses the distance correlation measure \mathcal{R} to select relevant information to predict influenza rate and applies the GLS procedure to the prediction of the influenza rate using readily available functional variables. These kinds of models are extremely useful to health managers in allocating resources in advance for an epidemic outbreak.

Keywords: Climatological variables, Dependent data, Functional data analysis, Influenza, Correlated errors.

Mathematics Subject Classification (2010): 62J12, 62M10, 62M20, 62P10.

1 Introduction

Influenza is an infectious disease with person-to-person transmission that characteristically occurs as an epidemic affecting the whole population, see for instance, Watson and Pebody (2012). The

¹Dept. of Statistics and Op. Res. Universidade de Santiago de Compostela, Spain.

²Instituto Tecnológico de Matemática Industrial (ITMATI), Spain.

³Dept. of Statistics and Op. Res., Universitat Politècnica de Catalunya, Spain.

⁴Dept. of Medicine. Universitat de Barcelona, Spain.

⁵CIBER en Epidemiología y Salud Pública (CIBERESP), Spain.

*Corresponding author. e-mail: manuel.oviedo@usc.es.

influenza virus has been categorized into types A, B and C. However influenza C is a mild disease without seasonality and is therefore not considered in influenza epidemics. One remarkable feature of the influenza A and B viruses is the frequency of changes in antigenicity. Alterations in the antigenic structure of the virus leads to infection by variants to which the population has little or no resistance.

The epidemiology of inter-pandemic influenza (also named seasonal influenza) is characterized in temperate zones by epidemics of variable size that occur during the colder winter months (November to April in the Northern Hemisphere and May to September in the Southern Hemisphere), each of which typically lasts 8-10 weeks (Van-Tam et al. (2012)). In a study on influenza activity throughout eight seasons (1999–2007), the average length of epidemics in 23 European countries was 15.6 weeks (median 15 weeks; range 12-19 weeks), see Paget et al. (2007).

The reasons for the seasonal presentation of epidemics are not entirely clear but they might result from more favorable environmental conditions for virus survival (Schaffer et al. (1976)). Various theories including improved virus survival in low temperatures, low humidity and low levels of ultraviolet radiation (Van-Tam et al. (2012)) have been advanced to explain this pattern in temperate zones. The typical incubation period for influenza is 1-4 days (average: 2 days).

Surveillance systems require accurate indicators that detect possible epidemics in advance. The epidemic of influenza is one of the problems of most concern to public health professionals across the world, due to its high levels of mortality and morbidity. Influenza is highly contagious and causes more morbidity than any other vaccine-preventable illness (Monto et al. (2002)). So accurate estimates of the incidence of influenza are essential, for both public health services and citizens, to provide advance warning of epidemics and allow preventive measures to reduce contagion.

Statistical methods to forecast the incidence of influenza in particular, and contagious diseases in general, have changed over time. In one of the first studies on time series, Choi and Thacker (1981) employed an ARIMA model to estimate pneumonia and influenza mortality. Dushoff et al. (2006) used a regression model to investigate how cold temperatures contribute to excess seasonal mortality. Höhle and Paul (2008) proposed an alternative model to monitor infectious diseases that consisted in applying count data charts to monitor time series. From a Bayesian framework, Conesa et al. (2015) proposed automated monitoring of influenza surveillance data that made it possible

to take the geographical component into account in statistical models in addition to temporal evolution. Contributions to this methodology are growing steadily through disease mapping. The studies by Ugarte et al. (2010) and Paul and Held (2011) are recent examples of this. Their common denominator is that they apply different statistical methodologies to multivariate time series (hierarchical Bayesian space–time, mixed models, P–splines and conditional autoregressive models (CAR), among others) of infectious disease counts, collected in different geographic areas, using multivariate or longitudinal data.

Functional data analysis (FDA) has grown in popularity over recent years alongside the increasing availability of continuous measurements in different contexts like Biomedicine (Cuevas et al. (2004)), Spectrometry (Ferraty and Vieu (2006)), Biology (Chiou et al. (2003)) and Medicine (Sørensen et al. (2013)), to mention only a few. This study extends the regression models for independent functional data to the case where the curves presents either spatial or temporal dependencies.

Our goal is to estimate the rate of influenza epidemics, using the information readily available from public sources possibly that include functional variables, by adapting or extending the GLS techniques from a multivariate framework to this new framework. So, our particular aim is to estimate the spatial or temporal dependence components of influenza, using regression models, and predict the rate of incidence of influenza for a horizon of 14 days (2 weeks). We initially model influenza using a traditional linear approach (with independent errors) and later extend these ideas to the functional case (with dependent errors).

The article is structured as follows. Section 2 presents the GLS approach for functional regression models. The estimation of the different parameters (for the regression function or the dependence) is usually done using maximum likelihood although, as an alternative, we introduce an iterative GLS (iGLS) procedure that provides similar results. The latter could be interesting when the structure of the dependence is complicated. The practical performances of the GLS and iGLS procedures are compared, by means of a simulation study (Section 3), to the case where the dependence is not considered. Section 4 applies these models to the prediction of the influenza rate in a region of Spain. Finally, Section 5 discusses the results obtained.

2 Methodology

The functional regression model (FRM) is one of the most studied topics in FDA over the last few years. A regression model is said to be “functional” if any of the variates involved (the predictors or the response) has a functional nature, i.e. it is a measure observed along a continuous interval. Cases with a scalar response and functional predictors have particularly attracted a lot of attention. For example, Sørensen et al. (2013) give a basic introduction for the analysis of functional data applied in datasets from medical science.

The functional regression model with scalar response (FRM) is stated as follows:

Let \mathcal{X}, Y two random variates taking values in $\mathcal{E} \times \mathbb{R}$ where \mathcal{E} is a functional space (semi-metric, normed or Hilbert). The relationship between the two variates can be expressed as follows:

$$Y = m(\mathcal{X}) + \epsilon = \mathbf{E}[Y|\mathcal{X}] + \epsilon \quad (1)$$

where ϵ is a real random variable verifying $\mathbf{E}[\epsilon|\mathcal{X}] = 0$. Depending on the nature of the functional space \mathcal{E} and on the regression operator m , we can classify the different types of FRM:

- **Multivariate Linear Model:** $\mathcal{E} = \mathbb{R}^p$ and m is the linear operator in the space, i.e. $\mathbf{E}[Y|\mathcal{X}] = \mathcal{X}\beta$ with $\beta \in \mathbb{R}^p$.
- **Functional Linear Model:** $\mathcal{E} = \mathcal{L}^2(T)$ is the Hilbert space of square integrable functions over T and m is a linear operator in the space, i.e. $m(\mathcal{X}) = \langle \mathcal{X}, \beta \rangle$ with $\beta \in \mathcal{L}^2(T)$. This model has been treated extensively in the literature mainly devoted to the optimal way of representing the linear operator through the representation of \mathcal{X} and β on a basis of $\mathcal{L}^2(T)$.

Depending on the latter, the references can be classified into two main categories:

- Fixed basis. The most commonly used basis in this context are the Fourier (see Ramsay and Silverman (2005)), the B-spline (see Cardot et al. (2003)) and the Wavelet (see for instance Antoniadis and Sapatinas (2003)).
- Data-driven basis. Two main basis computed from the data are used in the literature: the most parsimonious one is given by the functional principal components (see Horváth and Kokoszka (2012) and Cardot et al. (1999)) and the one that maximizes the covariance among the response and the functional predictor uses the functional partial

least square components (PLS) (see for instance Cardot et al. (2007) and Preda and Saporta (2005)).

Note that, due to the representation employed, the FRM is always an approximated model and its goodness typically relies on the properties of the chosen basis and its suitability to the data at hand.

- **Functional Non Linear Model:** \mathcal{E} is (at least) a semi-metric space and m is a continuous operator i.e. $\lim_{\mathcal{X}' \rightarrow \mathcal{X}} m(\mathcal{X}') = m(\mathcal{X})$. For a complete review of this model see Ferraty and Vieu (2006) and the references therein.
- **Extensions of the above models:** The above models could be extended in several ways, usually considering more than one predictive variate. This could lead to semi-linear models (Aneiros-Pérez and Vieu (2006, 2008)), additive models (Müller and Yao (2008), Ferraty and Vieu (2009), Febrero-Bande and González-Manteiga (2013)), single index models (Chen et al. (2011), Goia (2012)) or projection pursuit models (Ferraty et al. (2013)).

Many of the above-mentioned authors consider that $\epsilon = (\epsilon_1, \dots, \epsilon_{n,s})'$ is an homoskedastic independent error vector, i.e. $\mathbf{E}[\epsilon] = 0, \text{Var}[\epsilon] = \sigma^2$ and $\text{Cov}(\epsilon_i, \epsilon_j) = 0, i \neq j$. This assumption is made to obtain simple diagnostics or confidence intervals for the response but it could be too restrictive in functional regression models and difficult to check or fulfill in practice. Some papers consider dependence in the functional variate. See, for example, Delicado et al. (2010), Giraldo et al. (2011) and Menafoglio et al. (2013) for contributions devoted to spatial dependence with functional data or Battey and Sancetta (2013), Besse et al. (2000), Damon and Guillas (2005) and Hörmann and Kokoszka (2010) for time dependence. In both cases, the functional nature of the variate complicates the predictive ability of the model. The aim of this paper is to extend the GLS approach (see for example Kariya and Kurata (2004)) to the functional context as the simplest way of incorporating temporal or spatial dependence in the regression models. In fact, the GLS approach can handle a wide range of regression models with dependence in a simple way: equi-correlation models, random effects, time and spatial dependence, and so on.

2.1 Functional Generalized Least Squares Regression

The functional generalized least squares regression (FGLS) model between two centered variables ($\mathbf{E}[y] = 0$, $\mathbf{E}[\mathcal{X}] = 0$) states that

$$y = \langle \mathcal{X}, \beta \rangle + \epsilon = \int_T \mathcal{X}(t)\beta(t)dt + \epsilon \quad (2)$$

where $\beta \in \mathcal{L}_2(T)$ and ϵ is now a random vector with mean 0 and covariance matrix $\Omega = \mathbf{E}[\epsilon\epsilon']$. This model includes, as its special cases, many others models, all of them based on $\Omega = \Omega(\theta) = \sigma^2\Sigma(\theta)$, where θ is the parameter associated with the dependence structure of Ω . Some classical examples are presented in the following models:

(a) Equi-correlated model: $\text{Var}[\epsilon_i] = \sigma^2$ and $\text{Cov}(\epsilon_i, \epsilon_j) = \sigma^2\theta, i \neq j, \theta \in (-1, 1)$

(b) Heteroskedastic block model: $\Omega = \text{diag}(\sigma_1^2\mathbf{I}_{n_1} | \sigma_2^2\mathbf{I}_{n_2} | \dots | \sigma_p^2\mathbf{I}_{n_p})$ with $n_1 + n_2 + \dots + n_p = n$

(c) AR(1) model: $\epsilon_i = \theta\epsilon_{i-1} + \varepsilon_i$ with $|\theta| < 1$, $\mathbf{E}[\varepsilon_i] = 0$, $\text{Var}[\varepsilon_i] = \tau^2$ and $\text{Cov}(\varepsilon_i, \varepsilon_j) = 0, i \neq j$

$$\Omega = \frac{\tau^2}{1 - \theta^2} (\theta^{|i-j|})_{i,j=1}^n$$

The variance structure is also known for every ARMA(p, q) model.

(d) Spatial correlation model:

$$\Omega = \sigma^2 (\rho(d(s_i, s_j)))$$

where s_i, s_j are, respectively, the locations for i, j ; and ρ is the spatial correlation function.

2.2 Estimation of FGLS

The classical theory of Kariya and Kurata (2004) can be extended to the functional case by adapting the GLS criterion accordingly, i.e.

$$GLS(\beta, \theta) = (y - \langle \mathcal{X}, \beta \rangle)' \Sigma(\theta)^{-1} (y - \langle \mathcal{X}, \beta \rangle)$$

Given the sample $\{(\mathcal{X}_1, y_1), \dots, (\mathcal{X}_{n,s}, y_{n,s})\}$, we can approximate \mathcal{X}_i and β using a finite sum of the basis elements:

$$\mathcal{X}_i(t) \approx \sum_k^{K_x} c_{ik} \psi_k(t), \quad \beta(t) \approx \sum_k^{K_\beta} b_k \varphi_k(t)$$

The preceding equations can be expressed as matrix notation using the evaluation in a grid of the length M $\{a = t_1 < \dots < t_M = b\}$ as

$$\mathbf{X} = \mathbf{C}\Psi, \quad \mathbf{B} = \mathbf{b}'\varphi$$

, where \mathbf{X} is the matrix $n \times M$ with the evaluations of the curves in the grid, \mathbf{C} is the matrix $n \times K_x$ with the coefficients of the representation in the basis and Ψ is the matrix $K_x \times M$ with the evaluations of the basis elements on the grid. Similarly, \mathbf{B} is the matrix $(1 \times M)$ with the evaluation of the β parameter on the grid, φ is the matrix $(K_\beta \times M)$ with the evaluations of the basis $\{\varphi_j\}$ and \mathbf{b} on the grid, is the vector of the coefficients of β in the basis.

With this notation, the terms $\{\langle \mathcal{X}_i, \beta \rangle\}_{i=1}^n$ can be approximated by $\mathbf{C}\Psi\varphi'\mathbf{b} = \mathbf{Z}\mathbf{b}$ which, in essence, is a reformulation of a classical multivariate linear model that approximates the functional model. Here, the matrix \mathbf{Z} takes into account all the approximation steps done with the information available: the chosen basis for \mathcal{X} and β with the selected components: K_x and K_β .

Once a certain approximation is selected, supposing that θ is known, we can define $\mathbf{W} = \Sigma(\theta)^{-1}$, and use the classical theory for multivariate GLS to obtain the BLUE of \mathbf{b} through:

$$\mathbf{b}_\Sigma = (\mathbf{Z}'\mathbf{W}\mathbf{Z})^{-1}\mathbf{Z}'\mathbf{W}y,$$

where \mathbf{b}_Σ has covariance

$$\text{Cov}(\mathbf{b}_\Sigma) = \sigma^2 (\mathbf{Z}'\mathbf{W}\mathbf{Z})^{-1}$$

Finally, the fitted values are obtained by:

$$\hat{y} = \mathbf{Z}(\mathbf{Z}'\mathbf{W}\mathbf{Z})^{-1}\mathbf{Z}'\mathbf{W}y = \mathbf{H}_\Sigma y$$

where \mathbf{H} is the hat matrix.

Once the model is estimated, we can compute the prediction in a new point $\{\mathcal{X}_0\}$ using the model chosen for Σ . Being $\Delta' = \text{Cov}(\epsilon, \epsilon_0)$ and $\Sigma_0 = \text{Cov}(\epsilon_0\epsilon_0')$, we can obtain the equations for prediction:

$$\begin{aligned} \hat{y}_0 &= \langle \mathcal{X}_0, \hat{\beta} \rangle + \Delta\Sigma^{-1} \left(y - \langle \mathcal{X}, \hat{\beta} \rangle \right) \\ \text{Var}[\hat{y}_0] &= \sigma^2 \left(\Sigma_0 - \Delta\Sigma^{-1}\Delta' \right) \end{aligned}$$

The GLS criterion can be employed to jointly estimate all the parameters associated to the model and can be expressed as:

$$\min_{K_x, K_\beta, \mathbf{b}, \theta} GLS = \min_{K_x, K_\beta, \mathbf{b}, \theta} (y - \mathbf{Z}\mathbf{b})' \Sigma(\theta)^{-1} (y - \mathbf{Z}\mathbf{b}),$$

where the parameters K_x and K_β related to the basis for \mathcal{X} and β are typically chosen *a priori* taking into account, for instance, the quality of the data and its representation on the discretization grid or other considerations related to the data-generating process (smoothness, physical restrictions, interpretability,...). The direct minimization of GLS usually cannot be affordable even though we only consider the parameters \mathbf{b} and θ . The generalized cross-validation (GCV) criterion has been widely used to this end despite not being the right criterion for dependent errors. We use the generalized correlated cross-validation (GCCV) as an alternative. This suggested criterion is an extension to GCV within the context of correlated errors proposed by Carmack et al. (2012). It is defined as follows:

$$GCCV(K_x, K_\beta, \mathbf{b}, \theta) = \frac{\sum_{i=1}^n (y_i - \hat{y}_{i,\mathbf{b}})^2}{\left(1 - \frac{\text{tr}(\mathbf{C})}{n}\right)^2}$$

where $\mathbf{C} = 2\mathbf{S}\Sigma(\theta) - \mathbf{S}\Sigma(\theta)\mathbf{S}'$ takes into account the effect of the dependence, the trace of \mathbf{C} is an estimation of the degrees of freedom consumed by the model and \mathbf{S} is the smoother matrix. The important advantage of this criterion is that it is rather easy to compute. It avoids the need to compute the inverse of the matrix Σ . Even so, the GLS criterion mostly depends on the structure of Σ and could be hard to minimize or computationally expensive. In these cases, the following iterative procedure (iGLS) is equivalent to the classical GLS.

- (1) Begin with a preliminary estimation of $\hat{\theta} = \theta_0$ (for instance, $\theta_0 = 0$). Compute \hat{W} .
- (2) Estimate $\mathbf{b}_\Sigma = (\mathbf{Z}'\hat{W}\mathbf{Z})^{-1}\mathbf{Z}'\hat{W}y$
- (3) Based on the residuals, $\hat{e} = (y - \mathbf{Z}\mathbf{b}_\Sigma)$, update $\hat{\theta} = \rho(\hat{e})$ where ρ depends on the dependence structure chosen.
- (4) Repeat steps 2 and 3 until convergence (small changes in \mathbf{b}_Σ and/or $\hat{\theta}$)

3 Simulation

We used two functional linear models (FLM) included in Cardot et al. (2003) to compare the effect of a temporal dependence. We specifically generate samples of size $n = 100$ from the FLM model $y = \langle \mathcal{X}, \beta \rangle + \epsilon$, \mathcal{X} being a Wiener process defined on $[0, 1]$ and ϵ an AR(1) process with parameter

ϕ and variance $\text{Var}[\epsilon] = \text{snr}^{-1} \text{Var}[\langle \mathcal{X}, \beta \rangle]$. The two models differ only in the β parameter that are respectively:

(a) $\beta(t) = 2 \sin(0.5\pi t) + 4 \sin(1.5\pi t) + 5 \sin(2.5\pi t), t \in [0, 1],$

(b) $\beta(t) = \log(15t^2 + 10) + \cos(4\pi t), t \in [0, 1].$

The scenario (a) corresponds to a β parameter which has an exact representation respect to the first three theoretical principal components (PC) of the Wiener process. On the contrary, the β parameter for scenario (b) cannot be well represented using a small number of PCs of the Wiener process. In both cases, we used principal components and B-splines to estimate the β parameter and we employed the same basis selected for β to represent \mathcal{X} .

	ϕ , PC				ϕ , BSP			
<i>snr</i>	0.0	0.3	0.6	0.9	0.0	0.3	0.6	0.9
0.05	3.76	3.85	3.99	3.69	6.92	6.87	7.09	6.34
0.10	3.69	3.63	3.87	3.63	6.54	6.71	6.88	6.01
0.20	3.51	3.52	3.66	3.58	6.29	6.18	6.53	5.79

Table 1: Average of number of basis elements selected by GCCV criterion.

Tables 1 to 4 summarizes the results for the first model (a) to show, respectively, the average number of selected components chosen using GCCV criterion, the mean square error (MSE) for estimation of β , the MSE for estimation of ϕ and the mean square prediction errors (MSPE) for horizons 1, 5 and 10 for the $B = 1,000$ replicas. In these results, LM denotes the estimation through a classical functional linear model whereas GLS and iGLS correspond, respectively, to the functional GLS and functional iGLS methods (shown in Section 2) for AR(1) dependent errors. We use the GCCV criterion to determine the number of FPC with a search range from 1 to 8. Table 1 shows an average number of FPC selected components between 3 and 4 with a slight tendency to lower values as the *snr* grows. The range for components using cubic B-splines is from 4 to 11, even though we have no theoretical quantity to compare it to, the average number of selected components is between 6 and 7. It seems that there are no trends with respect to

¹Signal to noise ratio

$$\mathbf{E} \left[\left\| \beta - \hat{\beta} \right\|^2 \right]$$

		ϕ , PC				ϕ , BSP			
<i>snr</i>	Model	0	0.3	0.6	0.9	0	0.3	0.6	0.9
0.05	LM	0.51	0.50	0.50	0.49	0.97	0.92	0.97	0.89
0.05	GLS	0.51	0.48	0.44	0.46	0.97	0.89	0.67	0.50
0.05	iGLS	0.51	0.48	0.45	0.47	0.97	0.86	0.66	0.49
0.10	LM	0.60	0.61	0.59	0.57	1.38	1.35	1.35	1.21
0.10	GLS	0.61	0.58	0.50	0.49	1.39	1.27	1.00	0.66
0.10	iGLS	0.61	0.58	0.51	0.50	1.38	1.23	0.93	0.67
0.20	LM	0.76	0.76	0.73	0.75	1.79	1.70	1.90	1.75
0.20	GLS	0.77	0.72	0.63	0.58	1.80	1.62	1.35	0.80
0.20	iGLS	0.77	0.71	0.61	0.56	1.80	1.58	1.30	0.78

Table 2: Mean square error of β parameter. Model (a)

the ϕ values. Table 2 clearly shows the advantage of the PC estimator over the B-splines. The estimation error using B-splines typically doubles the error using PCs.

$$\mathbf{E} \left[\left(\phi - \hat{\phi} \right)^2 \right]$$

		ϕ , PC				ϕ , BSP			
<i>snr</i>	Model	0	0.3	0.6	0.9	0	0.3	0.6	0.9
0.05	GLS	0.005	0.005	0.003	0.002	0.006	0.005	0.003	0.001
0.05	iGLS	0.006	0.005	0.003	0.002	0.006	0.005	0.003	0.001
0.10	GLS	0.005	0.004	0.004	0.002	0.005	0.004	0.004	0.001
0.10	iGLS	0.005	0.004	0.004	0.002	0.006	0.004	0.004	0.002
0.20	GLS	0.006	0.004	0.003	0.002	0.006	0.004	0.003	0.001
0.20	iGLS	0.006	0.004	0.003	0.002	0.006	0.004	0.003	0.002

Table 3: Mean square error of ϕ parameter. Model (a)

$$MSPE = \sum_{i=1}^B (y_{n+h} - \hat{y}_{n+h})^2$$

		ϕ	0			0.3			0.6			0.9		
<i>snr</i>	Model	<i>h</i>	1	5	10	1	5	10	1	5	10	1	5	10
0.05	LM.PC		0.07	0.07	0.07	0.07	0.08	0.07	0.09	0.08	0.08	0.07	0.07	0.08
0.05	GLS.PC		0.07	0.07	0.07	0.07	0.08	0.07	0.05	0.07	0.07	0.02	0.05	0.07
0.05	iGLS.PC		0.07	0.07	0.07	0.07	0.08	0.07	0.05	0.07	0.07	0.02	0.05	0.07
0.05	LM.BSP		0.07	0.08	0.07	0.07	0.08	0.07	0.09	0.08	0.08	0.07	0.07	0.08
0.05	GLS.BSP		0.07	0.08	0.08	0.07	0.08	0.07	0.05	0.07	0.08	0.01	0.05	0.07
0.05	iGLS.BSP		0.07	0.08	0.08	0.07	0.08	0.07	0.05	0.07	0.08	0.01	0.05	0.07
0.10	LM.PC		0.18	0.18	0.15	0.16	0.16	0.16	0.17	0.17	0.18	0.15	0.16	0.18
0.10	GLS.PC		0.18	0.18	0.15	0.14	0.16	0.16	0.11	0.16	0.17	0.04	0.12	0.17
0.10	iGLS.PC		0.18	0.18	0.15	0.14	0.16	0.16	0.11	0.16	0.17	0.04	0.11	0.16
0.10	LM.BSP		0.18	0.18	0.15	0.16	0.16	0.16	0.17	0.17	0.18	0.16	0.17	0.18
0.10	GLS.BSP		0.18	0.18	0.15	0.15	0.16	0.15	0.12	0.16	0.18	0.04	0.12	0.16
0.10	iGLS.BSP		0.18	0.18	0.15	0.15	0.16	0.15	0.12	0.16	0.18	0.04	0.11	0.16
0.20	LM.PC		0.33	0.40	0.38	0.37	0.35	0.34	0.36	0.35	0.39	0.37	0.38	0.39
0.20	GLS.PC		0.32	0.40	0.38	0.34	0.35	0.34	0.24	0.34	0.38	0.07	0.24	0.32
0.20	iGLS.PC		0.32	0.40	0.38	0.34	0.35	0.34	0.24	0.34	0.38	0.07	0.24	0.32
0.20	LM.BSP		0.34	0.41	0.39	0.38	0.38	0.34	0.38	0.37	0.40	0.38	0.39	0.40
0.20	GLS.BSP		0.34	0.42	0.39	0.35	0.38	0.34	0.25	0.34	0.39	0.08	0.25	0.33
0.20	iGLS.BSP		0.34	0.42	0.39	0.35	0.38	0.34	0.25	0.34	0.39	0.08	0.25	0.32

Table 4: Mean square prediction errors for different lags.

In this table, we can also see the improved estimates of the GLS and IGLS method over the LM, especially when ϕ grows. The same equivalence is shown in Table 3 for the mean square error (MSE) of the ϕ parameter, which shows better results as the dependence grows. Finally, Table 4 shows the mean square prediction errors (MSPE) for different lags showing a clear improvement of GLS procedures, specially for large ϕ and shorter lags. With respect to the prediction ability between PC or B-splines, the results show that both methods are almost equivalent with minor

differences along the table.

4 Real example: flu prediction

Galicia is a region of 29,574 km² located in Northwest Spain with a population of 2.8 million people. We analyzed the weekly incidence of reported cases of influenza in Galicia between 2001 and 2011 for each of 53 Galician counties.

$$\text{Rate}_{n,s} = \log(\text{cases}_{n,s} \times 100000 / \text{pop}_{n,s})$$

for county s and week n . The Statistical Institute of Galicia (IGE, <http://www.ige.eu>) provided population (pop) and the Health Department of Galicia (www.sergas.es) provided the number of cases of influenza ($cases$).

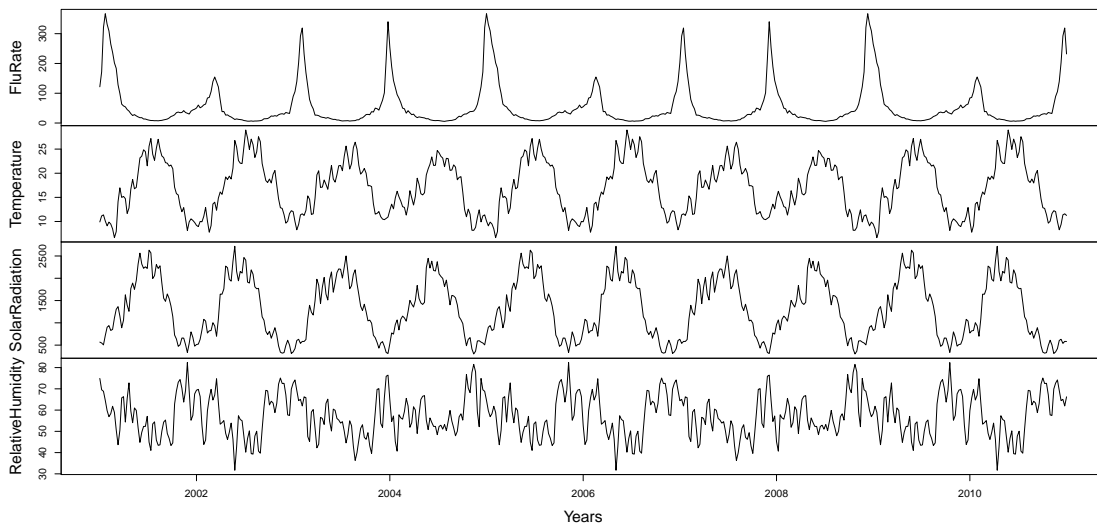


Figure 1: From top to bottom: Weekly influenza rate, and daily average temperature, solar radiation and relative humidity in the Galician region during the period.

The influenza season in Galicia begins in week 40 and ends in week 20 of the following year. The goal is to predict the incidence of influenza for the following two weeks ($n + 1$ and $n + 2$) in the s regions with the available information:

- $\text{Rate}_{n,s}(w)$: Weekly influenza rate for last 13 weeks, $w \in [n - 12, n]$.
- $\text{Temp}_{n,s}(t)$: Daily temperature in Celsius degrees ($^{\circ}\text{C}$) for last 14 days, $t \in [n - i/7, n]$, for $i = 14, \dots, 1$.
- Dushoff et al. (2006) defined cold as the number of degrees below a threshold temperature: $\text{Temp.thres}_{n,s} = \min(\text{Temp}_{n,s} - \text{thres}, 0)$ with $\text{thres} = 10^{\circ}\text{C}$. The functional variable is defined as: $\text{Temp.thres}_{n,s}(t)$ with $t \in [n - i/7, n]$, for $i = 14, \dots, 1$.
- $\text{SR}_{n,s}(t)$: Daily solar radiation (W/m^2) for the last 14 days, $t \in [n - i/7, n]$, for $i = 14, \dots, 1$.
- $\text{Hum}_{n,s}(t)$: Relative humidity for the last 14 days: , $t \in [n - i/7, n]$, for $i = 14, \dots, 1$.

Figure 1 shows that influenza normally starts in the late autumn and reaches a peak at the beginning of the calendar year. These plots clearly show the large difference between reported influenza cases in winter and summer. We downloaded meteorological data from the regional Weather Service of Galicia (<http://www.meteogalicia.es/>).

4.1 Variable Selection using Distance Correlation Measure

Distance correlation \mathcal{R} is a measure of dependence between random vectors introduced by Székely et al. (2007). The distance correlation satisfies $0 < \mathcal{R}(X, Y) < 1$ and its interpretation is similar to the squared Pearson's correlation. However, the advantages of distance correlation over the Pearson correlation is that it defines $\mathcal{R}(X, Y)$ in arbitrary finite dimensions of X and Y and \mathcal{R} characterises independence, i.e. $\mathcal{R}(X, Y) = 0 \Leftrightarrow X, Y$ are independent. Recently, Lyons (2013) provided conditions for the application of the distance correlation to functional spaces. So, this measure seems to be a good indicator of the correlations between functional and multivariate variables that may be useful for designing a functional linear model (for instance, avoiding variates with high collinearity). We can easily calculate the empirical distance correlation $\mathcal{R}_{n,s}(\mathbf{X}, \mathbf{Y})$ as

$$\mathcal{R}_{n,s}(\mathbf{X}, \mathbf{Y}) = \sqrt{\frac{\mathcal{V}_{n,s}^2(\mathbf{X}, \mathbf{Y})}{\sqrt{\mathcal{V}_{n,s}^2(\mathbf{X})\mathcal{V}_{n,s}^2(\mathbf{Y})}}}$$

where $\mathcal{V}_{n,s}(\mathbf{X}, \mathbf{Y})$ is the empirical distance covariance defined by $\mathcal{V}_{n,s}^2(\mathbf{X}, \mathbf{Y}) = \frac{1}{n^2} \sum_{k,l=1}^n A_{kl}B_{kl}$ where $A_{kl} = a_{kl} - \bar{a}_{k.} - \bar{a}_{.l} + \bar{a}_{..}$ and $B_{kl} = b_{kl} - \bar{b}_{k.} - \bar{b}_{.l} + \bar{b}_{..}$ with $a_{kl} = \|X_k - X_l\|$, $b_{kl} =$

$\|Y_k - Y_l\|$, $k, l = 1, \dots, n$, and the subscript \cdot denotes that the mean is computed for the index that it replaces. Similarly, $\mathcal{V}_{n,s}(\mathbf{X})$ is the non-negative number defined by $\mathcal{V}_{n,s}^2(\mathbf{X}) = \mathcal{V}_{n,s}^2(\mathbf{X}, \mathbf{X}) = \frac{1}{n^2} \sum_{k,l=1}^n A_{kl}^2$.

We used the distance correlation measure \mathcal{R} to select the information relevant to the prediction of influenza rate. The results are shown in Table 5. Relative humidity $\text{Hum}_{n,s}(t)$ is the variable that has the lowest correlation with the influenza rate $\{\text{Rate}_{n+1,s}, \text{Rate}_{n+2,s}\}$ and therefore the set of possible predictor variables is reduced to: $\{\text{Rate}_{n,s}(w), \text{Temp}_{n,s}(t), \text{Temp.thres}_{n,s}(t), \text{SR}_{n,s}(t)\}$. Besides, the distance correlation values lead to designing the models avoiding closely related covariates closely related (for instance, $\text{Temp}_{n,s}(t)$ and $\text{Temp.thres}_{n,s}(t)$) and thereby reduces the number of possible models tested.

\mathcal{R}	$\text{Rate}_{n,s}(w)$	$\text{Temp}_{n,s}(t)$	$\text{Temp.thres}_{n,s}(t)$	$\text{SR}_{n,s}(t)$	$\text{Hum}_{n,s}(t)$	$\text{Rate}_{n+1,s}$	$\text{Rate}_{n+2,s}$
$\text{Rate}_{n,s}(w)$	1.00	0.49	0.42	0.40	0.24	0.67	0.61
$\text{Temp}_{n,s}(t)$	0.49	1.00	0.89	0.82	0.53	0.49	0.46
$\text{Temp.thres}_{n,s}(t)$	0.42	0.89	1.00	0.72	0.43	0.41	0.41
$\text{SR}_{n,s}(t)$	0.40	0.82	0.72	1.00	0.70	0.50	0.50
$\text{Hum}_{n,s}(t)$	0.24	0.53	0.43	0.70	1.00	0.29	0.27

Table 5: Distance correlation \mathcal{R} between the response at week $n + 1$ and $n + 2$ and functional covariates at week n .

4.2 Prediction using temporal dependence structure

We employed a rolling analysis to compare the models in a predictive scenario. In our case, we initially split the data into an estimate sample of length $j = 1, \dots, n = 104$ weeks (2 years) in $s = 53$ counties and evaluated a predictive sample size in next two weeks $n + 1$ and $n + 2$ in the $s = 53$ counties. The rolling was performed along the epidemic periods for 2 years ($J = 40$ weeks) by computing the mean square prediction error: $MSPE = \frac{1}{n+J} \sum_{j=n+1}^{n+J} \frac{1}{s} \sum_{r=1}^s \left(\text{Rate}_{j,r} - \widehat{\text{Rate}}_{j,r} \right)^2$. For ease of simplicity, we employed the functional GLS procedure was employed simple autoregressive structure of order one AR(1). Therefore the elements k, l of the correlation matrix consists in $\Sigma_{k,l} = \sigma\phi^{|k-l|}$.

Table 6 summarises the predictive errors (MSPE) for the influenza season. The gain of the FGLS, in terms of MSPE, with the predictor $\text{Rate}_{n,s}(w)$ (models (a), (e), (f) and (g)) is relatively small

Model	Covariates	$n + 1$		$n + 2$	
		FLM	FGLS	FLM	FGLS
(a)	Rate $_{n,s}(w)$	0.56	0.49	0.86	0.83
(b)	Temp $_{n,s}(t)$	1.96	0.46	2.02	0.79
(c)	Temp.thres $_{n,s}(t)$	2.57	0.50	2.53	0.80
(d)	SR $_{n,s}(t)$	1.48	0.46	1.58	0.77
(e)	Rate $_{n,s}(w)$, Temp $_{n,s}(t)$	0.64	0.53	0.91	0.86
(f)	Rate $_{n,s}(w)$, Temp.thres $_{n,s}(t)$	0.67	0.57	0.92	0.87
(g)	Rate $_{n,s}(w)$, SR $_{n,s}(t)$	0.57	0.50	0.85	0.84
(h)	Temp $_{n,s}(t)$, SR $_{n,s}(t)$	1.85	0.48	1.93	0.83

Table 6: Serial prediction errors (MSPE) for influenza seasonal period using the rolling procedure.

with respect to considering FLM models. However, meteorological models such as models (b), (c), (d) and (h), the GLS setting reduces prediction error, at least, to one half. In the FGLS estimation the serial dependence considered is a quite simple AR(1). The $\hat{\phi}$ parameter ranges for 0.85 to 0.9 for meteorological models against 0.5 to 0.55 for models including the Rate as a covariate. The latter case is expected because the Rate $_{n,s}(w)$ accounts for part of the temporal dependence. The best models (b) and (d) with FGLS show small differences between them. The model (h) does not improve the results of models (b) and (d) in terms of MSPE. In fact it worsens them and this is probably due to collinearity. Among the models (b) and (d), the first is preferable because it is easier to interpret. Besides, solar radiation is often hard to obtain and depends on specialised devices whereas the covariates related to temperature are readily available with quite standard equipment.

Indeed, between the two temperature-related variables, the $\hat{\beta}$ parameter associated with the temperature Temp $_{n,s}(t)$ has a nicer interpretation. To this end, we have computed for models (a), (b) (c) and (d), the quantities $v_i = \langle \mathcal{X}_i, \hat{\beta} \rangle$ that include the contribution of each variable to the prediction of the influenza rate. We used these contributions to determine the pattern of curves that most influenced the increase and decrease in the incidence rate. Figure 2 shows the pattern of curves that most contributed to increasing (in red scale) and decreasing (in blue scale) the influenza rate. In particular, we split the data with respect to the quartiles of v_i and computed the average functional variate for each group (blue, sky blue, red and dark red, respectively corre-

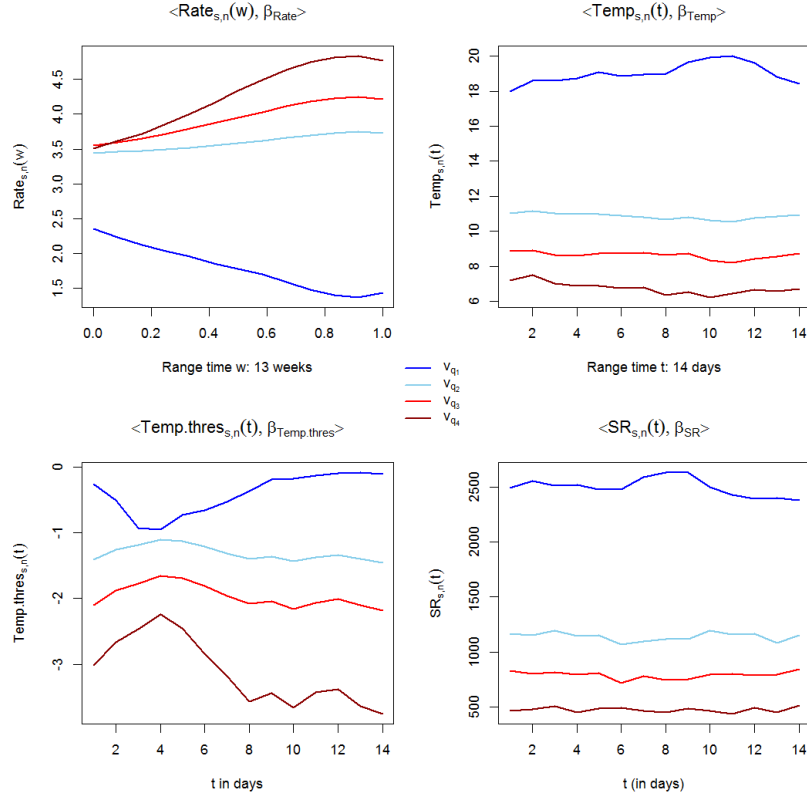


Figure 2: Shape of rate curves (on left) and temperature threshold curves (on right) in function of their projection value $v_X = \langle X, \hat{\beta} \rangle$. Average of curves: in 1st quartile of v_x (dark blue line), in 2nd quartile of v_x (blue line), in 3rd quartile of v_x (red line) and in 4th quartile of v_x (dark red line).

spond to quantile groups $[0, 0.25]$, $[0.25, 0.5]$, $[0.5, 0.75]$ and $[0.75, 1]$. This assesses the evaluation of the contribution of these curves in the response.

As the temperature increases (top left of Figure 2), the curves around 7°C (dark red line correspond to v_{q4} which is the highest contribution) provide an increase of the estimated influenza rate. In contrast, the contribution of the curves around 19°C have no impact on the influenza rate (blue line correspond v_{q1} , low or null contribution). The interpretation of the other models is straightforward.

5 Conclusion

This paper extends the GLS model from a multivariate to a functional framework: it thereby allows us to estimate functional regression models with temporal or spatial covariance errors structure in a simple way. It proposes an iterative version of the GLS estimator, that can help to model very complicated dependence structures. This procedure (called iGLS) is much simpler than GLS in terms of the optimization function to be accomplished but, of course, it may take longer due to the iterations. However, iGLS may be the only option when the sample size or the dimension of the parameter increases and the joint optimization performed by GLS is not affordable (in terms of complexity or memory consumption).

A simulation study shows that the GLS estimators improve the classical approach because they provide better estimations of the parameters associated with the regression model and extremely good results from the predictive point of view, specially for short lags.

We applied the GLS procedure to the prediction of the influenza rate using readily available functional variables. These kinds of models are extremely useful to health managers in allocating resources in advance for an epidemic outbreak. In particular, the nice interpretation of the model shows that influenza may increase due to a cold wave with daily temperatures of around 7°C for two weeks.

In our example, the error structure is estimated by a simple AR(1) and it obtains a good fit for time dependence. We have also tried other ARMA models that have rendered similar results. Our method can additionally be used to explore more complex dependence structures like heterogeneous covariances by counties or even spatio-temporal modelling.

Our results are consistent with much of the literature on influenza. By simply using the temperature variables that are easy to obtain, the model achieves results akin to those of models with variables that are more difficult to measure. Our results also show that the temporal dependence of the influenza virus is strong and stable over time. Future studies could extend generalized mixed models to the functional framework.

Acknowledgments

This research was partially supported by the Spanish Ministerio de Ciencia y Tecnología, grant MTM2013-41383-P. The authors thanks the healthcare provider: the Service Epidemiology of the Dirección Xeral de Saúde Pública (SERGAS) from the Consellería de Sanidade (Xunta de Galicia).

References

- Aneiros-Pérez, G. and Vieu, P. (2006). Semi-functional partial linear regression. *Statistics & Probability Letters*, 76(11):1102–1110.
- Aneiros-Pérez, G. and Vieu, P. (2008). Nonparametric time series prediction: A semi-functional partial linear modeling. *Journal of Multivariate Analysis*, 99(5):834–857.
- Antoniadis, A. and Sapatinas, T. (2003). Wavelet methods for continuous-time prediction using hilbert-valued autoregressive processes. *Journal of Multivariate Analysis*, 87(1):133–158.
- Battey, H. and Sancetta, A. (2013). Conditional estimation for dependent functional data. *Journal of Multivariate Analysis*, 120:1–17.
- Besse, P. C., Cardot, H., and Stephenson, D. B. (2000). Autoregressive forecasting of some functional climatic variations. *Scandinavian Journal of Statistics*, 27(4):673–687.
- Cardot, H., Ferraty, F., and Sarda, P. (1999). Functional linear model. *Statistics & Probability Letters*, 45(1):11–22.
- Cardot, H., Ferraty, F., and Sarda, P. (2003). Spline estimators for the functional linear model. *Statistica Sinica*, 13(3):571–592.
- Cardot, H., Mas, A., and Sarda, P. (2007). Clt in functional linear regression models. *Probability Theory and Related Fields*, 138(3):325–361.
- Carmack, P. S., Spence, J. S., and Schucany, W. R. (2012). Generalised correlated cross-validation. *Journal of Nonparametric Statistics*, 24(2):269–282.

- Chen, D., Hall, P., and Müller, H. G. (2011). Single and multiple index functional regression models with nonparametric link. *The Annals of Statistics*, 39(3):1720–1747.
- Chiou, J. M., Müller, H. G., and Wang, J. L. (2003). Functional quasi-likelihood regression models with smooth random effects. *Journal of the Royal Statistical Society: Series B (Statistical Methodology)*, 65(2):405–423.
- Choi, K. and Thacker, S. B. (1981). An evaluation of influenza mortality surveillance, 1962–1979 i. time series forecasts of expected pneumonia and influenza deaths. *American journal of epidemiology*, 113(3):215–226.
- Conesa, D., Martínez-Beneito, M., Amorós, R., and López-Quílez, A. (2015). Bayesian hierarchical poisson models with a hidden markov structure for the detection of influenza epidemic outbreaks. *Statistical methods in medical research*, 24(2):206–223.
- Cuevas, A., Febrero, M., and Fraiman, R. (2004). An anova test for functional data. *Comput. Statist. Data Anal.*, 47(1):111–122.
- Damon, J. and Guillas, S. (2005). Estimation and simulation of autoregressive hilbertian processes with exogenous variables. *Statistical inference for stochastic processes*, 8(2):185–204.
- Delicado, P., Giraldo, R., Comas, C., and Mateu, J. (2010). Statistics for spatial functional data: some recent contributions. *Environmetrics*, 21(3-4):224–239.
- Dushoff, J., Plotkin, J. B., Viboud, C., Earn, D. J., and Simonsen, L. (2006). Mortality due to influenza in the United States—an annualized regression approach using multiple-cause mortality data. *American Journal of Epidemiology*, 163(2):181–187.
- Febrero-Bande, M. and González-Manteiga, W. (2013). Generalized additive models for functional data. *Test*, 22(2):278–292.
- Febrero-Bande, M. and Oviedo de la Fuente, M. (2012). Statistical computing in functional data analysis: the R package fda.usc. *J. Statist. Software*, 51(4):1–28.
- Ferraty, F., Goia, A., Salinelli, E., and Vieu, P. (2013). Functional projection pursuit regression. *Test*, 22(2):293–320.

- Ferraty, F. and Vieu, P. (2006). *Nonparametric functional data analysis: theory and practice*. Springer.
- Ferraty, F. and Vieu, P. (2009). Additive prediction and boosting for functional data. *Comput. Statist. Data Anal.*, 53(4):1400–1413.
- Giraldo, R., Delicado, P., and Mateu, J. (2011). Ordinary kriging for function-valued spatial data. *Environmental and Ecological Statistics*, 18(3):411–426.
- Goia, A. (2012). A functional linear model for time series prediction with exogenous variables. *Statistics & Probability Letters*, 82(5):1005–1011.
- Höhle, M. and Paul, M. (2008). Count data regression charts for the monitoring of surveillance time series. *Computational Statistics & Data Analysis*, 52(9):4357–4368.
- Hörmann, S. and Kokoszka, P. (2010). Weakly dependent functional data. *The Annals of Statistics*, 38(3):1845–1884.
- Horváth, L. and Kokoszka, P. (2012). *Inference for functional data with applications*, volume 200. Springer.
- Kariya, T. and Kurata, H. (2004). *Generalized least squares*. Wiley.
- Lyons, R. (2013). Distance covariance in metric spaces. *The Annals of Probability*, 41(5):3284–3305.
- Menafoglio, A., Secchi, P., Dalla Rosa, M., et al. (2013). A universal kriging predictor for spatially dependent functional data of a hilbert space. *Electronic Journal of Statistics*, 7:2209–2240.
- Monto, A. S., Pichichero, M. E., Blanckenberg, S. J., Ruuskanen, O., Cooper, C., Fleming, D. M., and Kerr, C. (2002). Zanamivir prophylaxis: an effective strategy for the prevention of influenza types a and b within households. *Journal of Infectious Diseases*, 186(11):1582–1588.
- Müller, H. and Yao, F. (2008). Functional additive models. *Journal of the American Statistical Association*, 103(484):1534–1544.

- Paget, J., Marquet, R., Meijer, A., and van der Velden, K. (2007). Influenza activity in europe during eight seasons (1999–2007): an evaluation of the indicators used to measure activity and an assessment of the timing, length and course of peak activity (spread) across europe. *BMC infectious diseases*, 7(1):1.
- Paul, M. and Held, L. (2011). Predictive assessment of a non-linear random effects model for multivariate time series of infectious disease counts. *Statistics in Medicine*, 30(10):1118–1136.
- Preda, C. and Saporta, G. (2005). Pls regression on a stochastic process. *Computational Statistics & Data Analysis*, 48(1):149–158.
- Ramsay, J. and Silverman, B. (2005). *Functional Data Analysis*. Springer.
- Schaffer, F., Soergel, M., and Straube, D. (1976). Survival of airborne influenza virus: effects of propagating host, relative humidity, and composition of spray fluids. *Archives of virology*, 51(4):263–273.
- Sørensen, H., Goldsmith, J., and Sangalli, L. M. (2013). An introduction with medical applications to functional data analysis. *Statistics in medicine*, 32(30):5222–5240.
- Székeley, G. J., Rizzo, M. L., and Bakirov, N. K. (2007). Measuring and testing dependence by correlation of distances. *Ann. Statist.*, 35(6):2769–2794.
- Ugarte, M., Goicoa, T., and Militino, A. (2010). Spatio-temporal modeling of mortality risks using penalized splines. *Environmetrics*, 21(3-4):270–289.
- Van-Tam, J., Sellwood, C., et al. (2012). *Epidemiology and clinical features of interpandemic influenza.*, pages 1–8. CABI.
- Watson, J. M. and Pebody, R. G. (2012). Influenza surveillance and pandemic requirements. *Pandemic influenza*, pages 9–16.

Appendix A. Source code

This section provides information on the procedures used in the study. All functions are included in version 1.4 of the `fda.usc` package (Febrero-Bande and Oviedo de la Fuente (2012)) of software R. The function `fregre.gls` (and `predict.fregre.gls`) estimates (and predicts) the functional regression model with correlated errors, function `fregre.igls` is an iterative version of the previous one, function `dcor.fdist` computes the distance correlation between multivariate and functional objects and function `GCCV.S` computes the GCCV criterion.

Appendix B: Simulation (b)

The results for Simulation (b) are summarised in Tables 7, 8, 9 and 10. For the sake of simplicity, the results from the iGLS method are not shown because, as in the previous case, the numbers are almost identical with GLS. In this second model, the estimation of β cannot be done efficiently with the eigenfunctions of the Wiener process and so, the PC method has no a clear advantage over the B-splines. The number of selected components in Table 7 is clearly low for PC and quite unstable for higher values of ϕ . This is also reflected in Table 8 where, especially for $\phi = 0.9$, the estimation error is lower for the B-spline procedure. Note that, the estimation error can be split in two parts: a systematic one due to the lack of representation of β using a particular basis and the approximation one due to the particular estimation of that basis representation with the data at hand. This also affects the estimation of the dependence parameter as it is shown in Table 9 where the mean square errors provided are larger than in the previous model. In any case, the mean square prediction errors in Table 10 are better for the GLS procedure than for the classical one.

	ϕ , PC				ϕ , BSP			
<i>snr</i>	0	0.3	0.6	0.9	0	0.3	0.6	0.9
0.05	2.02	2.13	2.37	4.00	5.90	5.70	5.86	6.00
0.10	1.59	1.63	1.94	3.10	5.82	5.41	5.77	5.85
0.20	1.29	1.27	1.49	2.29	5.72	5.85	5.80	5.79

Table 7: Average of number of basis elements selected by GCCV criterion. Model (b).

$$\mathbf{E} \left[\left\| \beta - \hat{\beta} \right\|^2 \right]$$

		ϕ , PC				ϕ , BSP			
<i>snr</i>	Model	0	0.3	0.6	0.9	0	0.3	0.6	0.9
0.05	LM	1.14	1.12	1.10	0.90	1.70	1.55	1.35	0.75
0.05	GLS	1.14	1.11	1.07	0.88	1.71	1.42	0.94	0.40
0.10	LM	1.19	1.18	1.16	1.02	2.50	2.26	1.93	1.02
0.10	GLS	1.19	1.18	1.12	0.98	2.50	2.02	1.26	0.47
0.20	LM	1.24	1.23	1.21	1.11	3.52	3.52	2.84	1.43
0.20	GLS	1.24	1.22	1.18	1.07	3.55	3.15	1.91	0.58

Table 8: Mean square error of β parameter. Model (b)

$$\mathbf{E} \left[\left(\phi - \hat{\phi} \right)^2 \right]$$

		ϕ , PC				ϕ , BSP			
<i>snr</i>	Model	0	0.3	0.6	0.9	0	0.3	0.6	0.9
0.05	GLS	0.011	0.011	0.011	0.019	0.012	0.011	0.007	0.005
0.10	GLS	0.009	0.010	0.009	0.011	0.011	0.010	0.007	0.004
0.20	GLS	0.011	0.010	0.010	0.014	0.012	0.011	0.008	0.004

Table 9: Mean square error of ϕ parameter. Model (b)

$$MSPE = \sum_{i=1}^B (y_{n+h} - \hat{y}_{n+h})^2$$

ϕ		0			0.3			0.6			0.9			
<i>snr</i>	Model	<i>h</i>	1	5	10	1	5	10	1	5	10	1	5	10
0.05	LM.PC		0.14	0.14	0.14	0.13	0.14	0.12	0.10	0.09	0.10	0.03	0.03	0.03
0.05	GLS.PC		0.14	0.14	0.14	0.12	0.14	0.12	0.07	0.09	0.10	0.01	0.02	0.03
0.05	LM.BSP		0.14	0.14	0.14	0.12	0.14	0.12	0.10	0.09	0.10	0.03	0.02	0.03
0.05	GLS.BSP		0.14	0.14	0.14	0.11	0.14	0.12	0.06	0.09	0.09	0.00	0.02	0.02
<hr/>														
0.10	LM.PC		0.34	0.33	0.28	0.28	0.28	0.26	0.21	0.20	0.21	0.06	0.06	0.07
0.10	GLS.PC		0.34	0.33	0.28	0.25	0.28	0.26	0.14	0.19	0.21	0.02	0.05	0.06
0.10	LM.BSP		0.34	0.34	0.29	0.28	0.28	0.27	0.21	0.20	0.22	0.06	0.06	0.07
0.10	GLS.BSP		0.35	0.34	0.29	0.25	0.28	0.26	0.14	0.19	0.21	0.01	0.04	0.06
<hr/>														
0.20	LM.PC		0.61	0.76	0.73	0.64	0.59	0.58	0.45	0.42	0.48	0.14	0.14	0.14
0.20	GLS.PC		0.60	0.76	0.73	0.58	0.58	0.58	0.30	0.41	0.47	0.04	0.10	0.12
0.20	LM.BSP		0.64	0.77	0.74	0.64	0.63	0.59	0.45	0.44	0.47	0.14	0.14	0.14
0.20	GLS.BSP		0.64	0.78	0.74	0.59	0.63	0.58	0.29	0.40	0.46	0.03	0.09	0.11

Table 10: Mean squared prediction error for different lags. Model (b)